arXiv:1410.0188v1 [hep-ex] 1 Oct 2014

Charm CP violation and mixing at Belle

Byeong Rok Ko (on behalf of the Belle Collaboration)
Korea University, SEOUL 136-713, Republic of Korea
E-mail: brko@hep.korea.ac.kr

Abstract. We present charm CP violation and mixing measurements at Belle. They are the first observation of $D^0 - \bar{D}^0$ mixing in e^+e^- collisions from $D^0 \to K^+\pi^-$ decays, the most precise mixing and indirect CP violation parameters from $D^0 \to K^0_S\pi^+\pi^-$ decays, and the time-integrated CP asymmetries in $D^0 \to \pi^0\pi^0$ and $D^0 \to K^0_S\pi^0$ decays. Our mixing measurement in $D^0 \to K^+\pi^-$ decays excludes the no-mixing hypothesis at the 5.1 standard deviation level. The mixing parameters $x = (0.56 \pm 0.19^{+0.03+0.06}_{-0.09-0.09})\%$, $y = (0.30 \pm 0.15^{+0.04+0.03}_{-0.05-0.06})\%$ and indirect CP violation parameters $|q/p| = (0.90^{+0.16+0.05+0.06}_{-0.15-0.04-0.05})$, $\arg(q/p) = (-6 \pm 11 \pm 3^{+3}_{-4})^\circ$ measured from $D^0 \to K^0_S\pi^+\pi^-$ decays, and the time-integrated CP asymmetries $A_{CP}^{D^0\to\pi^0\pi^0} = (-0.03 \pm 0.64 \pm 0.10)\%$ and $A_{CP}^{D^0\to K^0_S\pi^0} = (-0.21 \pm 0.16 \pm 0.07)\%$ are the most precise measurements to date. Our measurements here are consistent with predictions of the standard model.

The magnitudes of CP violation (CPV) and mixing rate in the charm system are very small in the standard model (SM) [1, 2]. Therefore, D^0-$\bar{D}^0$ mixing and CPV measurements provide a unique probe to search for physics beyond the SM [3, 4]. $D^0 - \bar{D}^0$ mixing occurs since the mass eigenstates D_1 and D_2 are different from the flavor eigenstates D^0 and $\bar{D}^0$. The mass eigenstates can be written in terms of the flavor eigenstates, namely, $|D_{1,2}\rangle = p|D^0\rangle \pm q|\bar{D}^0\rangle$. The phenomenology of meson mixing is described by two parameters, $x = \Delta m/\Gamma$ and $y = \Delta\Gamma/2\Gamma$, where Δm and $\Delta\Gamma$ are the mass and width differences between the two mass eigenstates, and Γ is the average decay width of the mass eigenstates. Indirect CPV parameters are $|q/p|$ and $\arg(q/p)$, where the former and the latter are responsible for CPV in mixing and that in interference between the decays with and without mixing, respectively.

In this proceedings, we present charm CPV and mixing measurements from the data recorded with the Belle detector [5] at the e^+e^- asymmetric-energy collider KEKB [6].

1. Mixing in $D^0 \to K^+\pi^-$ decays

We present the first observation of $D^0 - \bar{D}^0$ mixing from an e^+e^- collision experiment by measuring the time-dependent ratio of the $D^0 \to K^+\pi^-$ (**W**rong **S**ign) to $D^0 \to K^-\pi^+$ (**R**ight **S**ign) decay rates [7]. Assuming CP conservation and that the mixing parameters are small ($|x| \ll 1$ and $|y| \ll 1$), the time-dependent RS and WS decay rates are $\Gamma_{\rm RS}(\tilde{t}/\tau) \approx |\mathcal{A}_{\rm CF}|^2 e^{-\frac{\tilde{t}}{\tau}}$ and $\Gamma_{\rm WS}(\tilde{t}/\tau) \approx |\mathcal{A}_{\rm CF}|^2 e^{-\frac{\tilde{t}}{\tau}}\left(R_D + \sqrt{R_D}y'\frac{\tilde{t}}{\tau} + \frac{x'^2+y'^2}{4}\left(\frac{\tilde{t}}{\tau}\right)^2\right)$, respectively, to second order in the mixing parameters, where $\tilde{t}$ is the true proper decay time, $\mathcal{A}_{\rm CF}$ is the **C**abibbo-**F**avored decay amplitude, τ is the D^0 lifetime, R_D is the ratio of DCS (**D**oubly **C**abibbo-**S**uppressed) to CF decay rates, $x' = x\cos\delta + y\sin\delta$, and $y' = y\cos\delta - x\sin\delta$, where δ is the strong phase difference

between the DCS and CF decay amplitudes. The time-dependent ratio of WS to RS decay rates then

$$R(t/\tau) = \frac{\int_{-\infty}^{+\infty} \Gamma_{\rm WS}(\tilde{t}/\tau)\mathcal{R}(t/\tau - \tilde{t}/\tau)d(\tilde{t}/\tau)}{\int_{-\infty}^{+\infty} \Gamma_{\rm RS}(\tilde{t}/\tau)\mathcal{R}(t/\tau - \tilde{t}/\tau)d(\tilde{t}/\tau)}, \quad (1)$$

where t is the reconstructed proper decay time and $\mathcal{R}(t/\tau - \tilde{t}/\tau)$ is the resolution function of the real decay time, $\tilde{t}$. Figure 1 shows the time-dependent ratios of WS to RS decays together with the two hypothesis tests, with (line) and without mixing (dots). The χ^2 difference between the "no-mixing" and "mixing" hypotheses, $\Delta\chi^2 = \chi^2_{\rm no-mixing} - \chi^2_{\rm mixing}$, is 29.3 for two degrees of freedom, corresponding to a probability of 4.3×10^{-7}; this implies the no-mixing hypothesis is excluded at the 5.1 standard deviation level. Thus, we observe $D^0 - \bar{D}^0$ mixing for the first time in an e^+e^- collision experiment. We also show this in Figure 2 with the 1σ, 3σ, and 5σ contours around the best fit point in the (x'^2, y') plane.

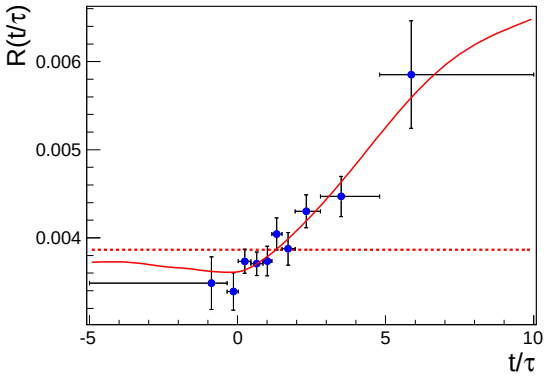

Figure 1. The time-dependent ratios of WS to RS decay rates. Points with error bars reflect the data and their total uncertainties. The lines show the fit with (solid) and without (dashed) the mixing hypothesis.

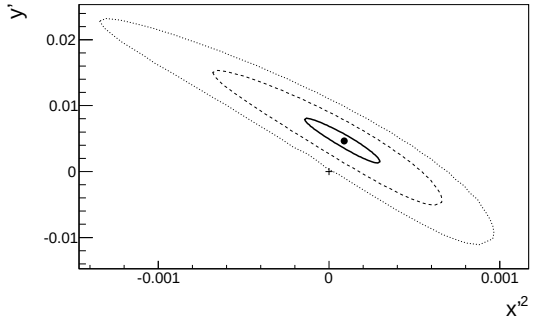

Figure 2. Best-fit point and contours in the (x'^2, y') plane. The solid, dashed, and dotted lines, respectively, correspond to 1, 3, and 5 standard Gaussian deviations from the best fit. The cross is the no-mixing point.

2. Mixing and indirect CPV in $D^0 \to K^0_S\pi^+\pi^-$ decays

We present the most precise mixing and indirect CP violation parameters from $D^0 \to K^0_S\pi^+\pi^-$ decays [8] using the time-dependent Dalitz fit analysis [9]. The time-dependent decay matrix elements of $D^0 \to K^0_S\pi^+\pi^-$ and $\bar{D}^0 \to K^0_S\pi^+\pi^-$ are

$$\begin{aligned} \mathcal{M}(m^2_+, m^2_-, t) &= g_+(t)\mathcal{A}(m^2_+, m^2_-) + \frac{q}{p}g_-(t)\bar{\mathcal{A}}(m^2_+, m^2_-) \text{ and} \\ \bar{\mathcal{M}}(m^2_+, m^2_-, t) &= g_+(t)\bar{\mathcal{A}}(m^2_+, m^2_-) + \frac{p}{q}g_-(t)\mathcal{A}(m^2_+, m^2_-), \end{aligned} \quad (2)$$

where $m^2_\pm = m^2_{K^0_S\pi^\pm}$, $\mathcal{A}(m^2_+, m^2_-) = \sum a_j e^{i\delta_i} A_j(m^2_+, m^2_-)$, $\bar{\mathcal{A}}(m^2_+, m^2_-) = \sum \bar{a}_j e^{i\bar{\delta}_i} A_j(m^2_+, m^2_-)$, $g_\pm(t) = (e^{-i\lambda_1 t} \pm e^{-i\lambda_2 t})/2$, and $\lambda_i = m_i - i\Gamma_i/2$, where a_j, δ_j, and $A_j(m^2_+, m^2_-)$ are amplitude, phase, and resonance matrix element, respectively. The decay matrix element squared $\mathcal{M}^2$ then contains the mixing parameters x and y as well as q/p of which magnitude and argument are indirect CPV parameters. Two separate time-integrated Dalitz fits to D^0 and $\bar{D}^0$ samples show no direct CPV resulting in $a_j \approx \bar{a}_j$ and $\delta \approx \bar{\delta}$. Hence, we search for indirect CPV assuming

no direct CPV, namely, $\mathcal{A}(m_+^2, m_-^2) = \bar{\mathcal{A}}(m_+^2, m_-^2)$. The best fit model for $\mathcal{A}(m_+^2, m_-^2)$ is found to be a sum of twelve Breit-Wigner for P- and D-wave resonances, K-matrix [10] and LASS [11] models for $\pi\pi$ and $K\pi$ S-wave states, respectively, without non-resonant decay. Figure 3 shows the proper-time distribution superimposing the fit under both direct and indirect CP conservation and the fit results are $x = (0.56 \pm 0.19^{+0.03+0.06}_{-0.09-0.09})\%$ and $y = (0.30 \pm 0.15^{+0.04+0.03}_{-0.05-0.06})\%$. With allowing indirect CPV, the fit returns $x = (0.56 \pm 0.19^{+0.04+0.06}_{-0.08-0.08})\%$, $y = (0.30 \pm 0.15^{+0.04+0.03}_{-0.05-0.07})\%$, $|q/p| = (0.90^{+0.16+0.05+0.06}_{-0.15-0.04-0.05})$, and $\arg(q/p) = (-6 \pm 11 \pm 3^{+3}_{-4})^\circ$. Our measurements of indirect CPV parameters are the most accurate to date, but consistent with no CPV. Figure 4 show the two-dimensional (x, y) confidence-level (C.L.) contours for the CP-conserved and CPV-allowed fits, where the no-mixing point $(x = 0, y = 0)$ is excluded with 2.5 standard deviations.

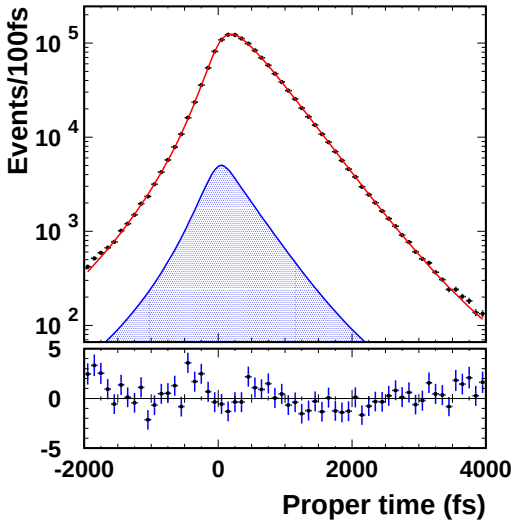

Figure 3. The proper-time distribution for events in the signal region (points) and fit projection for the CP conserved fit (curve). The shaded region shows the combinatorial components. The residuals are shown below the plot.

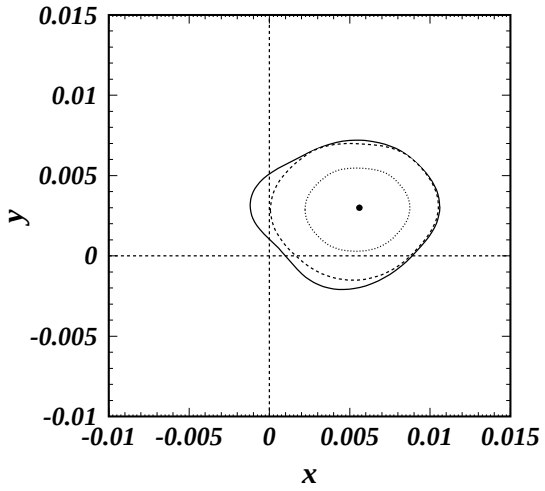

Figure 4. Central value (point) and C.L. contours for (x, y) : dotted (dashed) corresponds to 68.3% (95%) C.L. contour for CP-conserved Dalitz fit, and solid corresponds to 95% C.L. contour for CPV-allowed fit with statistical, experimental and model uncertainties included.

3. Time-integrated CPV in $D^0 \to \pi^0\pi^0$ and $D^0 \to K^0_S\pi^0$ decays

We present the time-integrated CPV asymmetry in $D^0 \to f$, $A_{CP}^{D^0 \to f}$, where f is the final state $\pi^0\pi^0$ or $K^0_S\pi^0$ [12]. It is measured through the reconstruction asymmetry

$$A_{\rm rec} = \frac{N_{\rm rec}^{D^{*+} \to D^0\pi_s^+} - N_{\rm rec}^{D^{*-} \to \bar{D}^0\pi_s^-}}{N_{\rm rec}^{D^{*+} \to D^0\pi_s^+} + N_{\rm rec}^{D^{*-} \to \bar{D}^0\pi_s^-}} \approx A_{CP}^{D^0 \to f} + A_{FB}^{D^{*+}} + A_\epsilon^{\pi_s^+} (+A_\epsilon^{\bar{K}^0}), \qquad (3)$$

where $N_{\rm rec}$ is the number of reconstructed signal events, A_{FB} is the forward-backward asymmetry, $A_\epsilon^{\pi_s^+}$ is the detection asymmetry between positively and negatively charged soft pions, and $A_\epsilon^{\bar{K}^0}$ is the asymmetry due to different nuclear interactions between $\bar{K}^0$ and K^0 [13], thus included to the decay $D^0 \to K^0_S\pi^0$. Once we remove $A_\epsilon^{\pi_s^+}$ with the correction in Ref. [14]

and $A_\epsilon^{\bar{K}^0}$ with the value in Ref. [15], then $A_{\rm rec}$ becomes to have $A_{CP}^{D^0\to f}$ and $A_{FB}^{D^{*+}}$ only, where the latter is an odd function of the cosine of the polar angle of the D^{*+} momentum in the center-of-mass system ($\cos\theta^*_{D^{*+}}$). Using the antisymmetry of $A_{FB}^{D^{*+}}$ in $\cos\theta^*_{D^{*+}}$, we obtain A_{CP} as a function of $|\cos\theta^*_{D^{*+}}|$ as shown in Figure 5. The central A_{CP} values obtained from a least-square minimization are $A_{CP}^{D^0\to\pi^0\pi^0} = (-0.03 \pm 0.64 \pm 0.10)\%$ and $A_{CP}^{D^0\to K^0_S\pi^0} = (-0.21 \pm 0.16 \pm 0.07)\%$ which are the most precise measurements to date revealing no CPV, thus consistent with the SM.

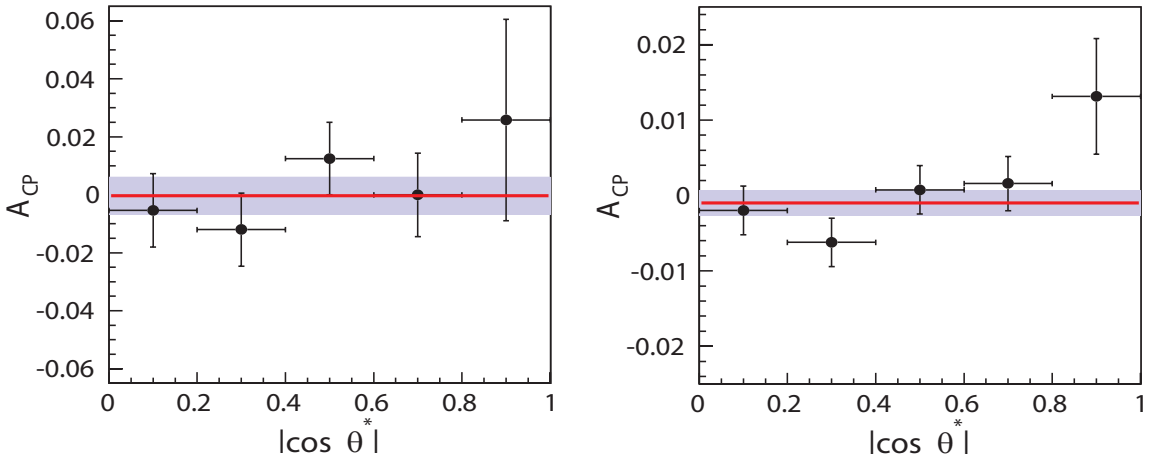

Figure 5. The A_{CP} values in the decays $D^0 \to \pi^0\pi^0$ (left) and $D^0 \to K^0_S\pi^0$ (right) as a function of $|\cos\theta^*|$. The solid lines and shaded regions represent the central value and 1σ interval of the A_{CP}.

Acknowledgments

B. R. Ko acknowledges support by NRF Grant No. NRF-2014R1A2A2A01005286.

References

[1] A. A. Petrov, Int. J. Mod. Phys. A **21**, 5686 (2006).
[2] A. F. Falk, Y. Grossman, Z. Ligeti, and A. A. Petrov, Phys. Rev. D **65**, 054034 (2002).
[3] E. Golowich, J. Hewett, S. Pakvasa, and A. A. Petrov, Phys. Rev. D **79**, 114030 (2009).
[4] Y. Grossman, A. L. Kagan, and Y. Nir, Phys. Rev. D **75**, 036008 (2007).
[5] A. Abashian *et al.* (Belle Collaboration), Nucl. Instrum. Meth. Phys. Res., Sect. A **479**, 117 (2002); also see the detector section in J. Brodzicka *et al.*, Prog. Theor. Exp. Phys. **2012**, 04D001 (2012).
[6] S. Kurokawa and E. Kikutani, Nucl. Instrum. Meth. Phys. Res., Sect. A **499**, 1 (2003), and other papers included in this volume; T. Abe *et al.*, Prog. Theor. Exp. Phys. **2013**, 03A001 (2013) and following articles up to 03A011.
[7] B. R. Ko *et al.* (Belle Collaboration), Phys. Rev. Lett. **112**, 111801 (2014).
[8] T. Peng *et al.* (Belle Collaboration), Phys. Rev. D **89**, 091103(R) (2014).
[9] D. M. Asner *et al.* (CLEO Collaboration), Phys. Rev. D **72**, 012001 (2005).
[10] V. V. Anisovich and A. V. Sarantsev, Eur. Phys. J. A **16**, 229 (2003).
[11] D. Aston *et al.* (LASS), Nucl. Phys. B **296**, 493 (1988).
[12] N. K. Nisar *et al.* (Belle Collaboration), Phys. Rev. Lett. **112**, 211601 (2014).
[13] B. R. Ko, E. Won, B. Golob, and P. Pakhlov, Phys. Rev. D **84**, 111501 (2011).
[14] B. R. Ko *et al.* (Belle Collaboration), Phys. Rev. Lett. **106**, 211801 (2011).
[15] B. R. Ko *et al.* (Belle Collaboration), Phys. Rev. Lett. **109**, 021601 (2012), [Erratum-ibid. **109**, 119903 (2012)].